Syntheses, Structures, and Properties of the Bis(cyclopentadienyl) Rare-Earth Imidodiphosphinochalcogenido Compounds $Cp_2Ln[N(QPPh_2)_2]$ (Ln = La, Gd, Er, or Yb for Q = Se; Ln = Yb for Q = S)

Christopher G. Pernin and James A. Ibers*

Department of Chemistry, Northwestern University, 2145 Sheridan Road, Evanston, Illinois 60208-3113

Received July 27, 1999

The compounds $Cp_2Ln[N(QPPh_2)_2]$ (Ln = La (**1**), Gd (**2**), Er (**3**), or Yb (**4**) for Q = Se, Ln = Yb (**5**) for Q = S) have been synthesized from the corresponding rare-earth tris(cyclopentadienyl) compound and $H[N(QPPh_2)_2]$. The structures of compounds **1**, **2**, **3**, and **5**, as determined by X-ray crystallography, consist of a Cp_2Ln fragment, coordinated η^3 through two chalcogen atoms and an N atom of the imidodiphosphinochalcogenido ligand $[N(QPPh_2)_2]^-$. In compound **4**, the Cp_2Yb moiety is coordinated η^2 through the two Se atoms of the $[N(SePPh_2)_2]^-$ ligand. ^{31}P and ^{77}Se (for **1**) NMR spectroscopies lend insight into the solution nature of these species. Crystal data: **1**, $C_{34}H_{30}LaNP_2Se_2$, triclinic, $P\bar{1}$, $a = 9.7959(10)$ Å, $b = 12.4134(13)$ Å, $c = 13.9077(14)$ Å, $\alpha = 88.106(2)°$, $\beta = 88.327(2)°$, $\gamma = 68.481(2)°$, $V = 1572.2(3)$ Å^3, $T = 153$ K, $Z = 2$, and $R_1(F) = 0.0257$ for the 5947 reflections with $I > 2\sigma(I)$; **2**, $C_{34}H_{30}GdNP_2Se_2$, triclinic, $P\bar{1}$, $a = 9.7130(14)$ Å, $b = 12.2659(17)$ Å, $c = 13.953(2)$ Å, $\alpha = 88.062(2)°$, $\beta = 87.613(2)°$, $\gamma = 69.041(2)°$, $V = 1550.7(4)$ Å^3, $T = 153$ K, $Z = 2$, and $R_1(F) = 0.0323$ for the 5064 reflections with $I > 2\sigma(I)$; **3**, $C_{34}H_{30}ErNP_2Se_2$, triclinic, $P\bar{1}$, $a = 9.704(2)$ Å, $b = 12.222(3)$ Å, $c = 13.980(4)$ Å, $\alpha = 88.230(4)°$, $\beta = 87.487(4)°$, $\gamma = 69.107(4)°$, $V = 1547.4(7)$ Å^3, $T = 153$ K, $Z = 2$, and $R_1(F) = 0.0278$ for the 6377 reflections with $I > 2\sigma(I)$; **4**, $C_{34}H_{30}NP_2Se_2Yb{\cdot}C_4H_8O$, triclinic, $P\bar{1}$, $a = 12.087(4)$ Å, $b = 12.429(4)$ Å, $c = 23.990(7)$ Å, $\alpha = 89.406(5)°$, $\beta = 86.368(5)°$, $\gamma = 81.664(5)°$, $V = 3558.8(18)$ Å^3, $T = 153$ K, $Z = 4$, and $R_1(F) = 0.0321$ for the 11 883 reflections with $I > 2\sigma(I)$; and **5**, $C_{34}H_{30}NP_2S_2Yb$, monoclinic, $P2_1/n$, $a = 13.8799(18)$ Å, $b = 12.6747(16)$ Å, $c = 17.180(2)$ Å, $\beta = 91.102(3)°$, $V = 3021.8(7)$ Å^3, $T = 153$ K, $Z = 4$, and $R_1(F) = 0.0218$ for the 6698 reflections with $I > 2\sigma(I)$.

Introduction

We recently reported the facile syntheses of two rare-earth chalcogenide species, namely $Cp_2Y[N(QPPh_2)_2]$ (Q = S, Se), from the protonolysis reaction of Cp_3Y with $HN(QPPh_2)_2$.[1] The compounds are isostructural, and each compound contains a Cp_2Y fragment attached η^3 through two chalcogen atoms and an N atom from the imidodiphosphinochalcogenido ligand, $[N(QPPh_2)_2]^-$. NMR spectroscopy indicates that the compounds retain their geometry in solution. The sulfur-containing compound is the first example of η^3-bonding from that ligand.

Since a convenient preparation of the ligand was published by Bhattacharyya and co-workers,[2−6] a variety of its coordination motifs have been uncovered. *Q*, *Q*′ coordination from the ligand is by far the most common motif, but others, such as multimetallic cluster compounds with bridging ligands, are known.[6−8] Our interest in the relatively underdeveloped area of soluble rare-earth chalcogenide compounds[9,10] prompted us to explore this ligand with the f-block metals.

In this paper, we extend our studies on Cp_2Ln (Ln = rare-earth element) coordinated to the $[N(QPPh_2)_2]^-$ ligand to include representatives of the early (La), middle (Gd), and late (Er, Yb) rare-earth elements to determine how their ionic radii affect the coordination mode of the ligand (see Scheme 1).

The compounds $Cp_2Ln[N(QPPh_2)_2]$ (Ln = La (**1**), Gd (**2**), Er (**3**), or Yb (**4**) for Q = Se; Ln = Yb (**5**) for Q = S) have been synthesized. The solid-state structures containing the selenide ligand indicate that the early and middle rare-earth elements accommodate η^3-coordination from the ligand, whereas the late and thus smaller Yb center shows η^2-coordination. To determine the effect of the chalcogen atom, the structure of the sulfide analogue of the Yb compound was also determined.

Experimental Section

General Procedures. All of the manipulations were carried out under strict exclusion of dioxygen and water with the use of standard Schlenk techniques.[11] Tetrahydrofuran (THF) was distilled from Na-benzophenone and bubbled with Ar for 10 min prior to use. Pentane was refluxed prior to being distilled over P_2O_5, and Ar gas was bubbled through it for 5 min before use. Cp_3Ln compounds were synthesized by a published

(1) Pernin, C. G.; Ibers, J. A. *Inorg. Chem.*, **1999**, *38*, 5478−5483.
(2) Bhattacharyya, P.; Woollins, J. D. *Polyhedron* **1995**, *14*, 3367−3388.
(3) Bhattacharyya, P.; Slawin, A. M. Z.; Williams, D. J.; Woollins, J. D. *J. Chem. Soc., Dalton Trans.* **1995**, 2489−2495.
(4) Bhattacharyya, P.; Slawin, A. M. Z.; Williams, D. J.; Woollins, J. D. *J. Chem. Soc., Dalton Trans.* **1995**, 3189−3193.
(5) Bhattacharyya, P.; Novosad, J.; Phillips, J.; Slawin, A. M. Z.; Williams, D. J.; Woollins, J. D. *J. Chem. Soc., Dalton Trans.* **1995**, 1607−1613.
(6) Bhattacharyya, P.; Slawin, A. M. Z.; Smith, M. B. *J. Chem. Soc., Dalton Trans.* **1998**, 2467−2475.
(7) Slawin, A. M. Z.; Ward, J.; Williams, D. J.; Woollins, J. D. *J. Chem. Soc., Chem. Commun.* **1994**, 421−422.
(8) Laguna, A.; Laguna, M.; Rojo, A.; Fraile, M. N. *J. Organomet. Chem.* **1986**, *315*, 269−276.
(9) Pernin, C. G.; Ibers, J. A. *Inorg. Chem.* **1997**, *36*, 3802−3803.
(10) Pernin, C. G.; Ibers, J. A. *J. Cluster Sci.* **1999**, *10*, 71−90.
(11) Shriver, D. F.; Drezdon, M. A. *Manipulation of Air-Sensitive Compounds*, 2nd ed.; Wiley: New York, 1986.

10.1021/ic990889o CCC: $19.00
Published on Web 02/25/2000

Scheme 1

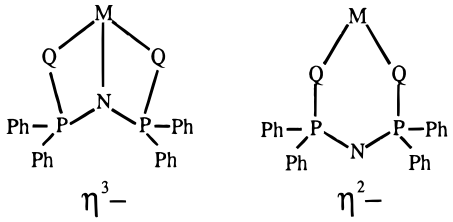

procedure[12] and stored in an Ar-filled glovebox before use. $HN(QPPh_2)_2$ was synthesized from $HN(PPh_2)_2$ and elemental chalcogen in a manner similar to previously published procedures.[3,5] NMR data on CD_2Cl_2 solutions of **1**, **2**, **3**, **4**, and **5** were recorded on either a 300 MHz Gemini spectrometer (^{31}P with a 5 mm NMR probe) or a 400 MHz Varian spectrometer (^{77}Se and ^{139}La with a 10 mm broad-band NMR probe) at 25 °C. ^{31}P chemical shifts, in ppm, were recorded at 120.470 MHz and were referenced to an external standard of 85% H_3PO_4 (set to 0 ppm). ^{77}Se chemical shifts, in ppm, were recorded at 76.295 MHz and referenced to an external standard of a saturated solution of Ph_2Se_2 in C_6D_6 (set to 460 ppm). The ^{139}La chemical shift, in ppm, was recorded at 56.494 MHz and referenced to a saturated solution of $LaCl_3$ in D_2O (set to 0 ppm). NMR collection parameters for compound **1**: 0.2 M CD_2Cl_2 solution; 5000 transients (^{77}Se) or 3708 transients (^{139}La); $d_1 = 1$ s; pulse width = 20 μs. UV−vis spectra for **3**, **4**, and **5** were recorded on a Cary spectrometer on approximately 1 mmol solutions in CH_2Cl_2.

$(C_5H_5)_2La[\eta^3\text{-}N(SePPh_2)_2]$, 1. White crystalline Cp_3La (100 mg, 0.12 mmol) and white powdered $HN(SePPh_2)_2$ (70 mg, 0.13 mmol) were loaded in separate flasks in an Ar-filled glovebox. The flasks were removed from the box and attached to a Schlenk line, where 10 mL of THF was added to each via syringe. The clear solution of the free acid was added over the course of 10 min, via cannulas, to the clear solution of Cp_3La, and the resulting clear solution was stirred for 1 h. The volume of this solution was reduced to 10 mL, and 10 mL of pentane was added. While sitting overnight at −15 °C, the solution produced large, clear colorless crystals of **1**, in addition to other compounds. Elemental analyses were never satisfactory for compound **1**, unlike the analyses for **2**, **3**, **4**, and **5** (see below). Mp: 274 °C. NMR: $^{31}P\{^1H\}$, major resonance at 37.1 ppm ($\Delta_{1/2} = 25$ Hz; $^1J_{P-Se} = 613$ Hz; $^2J_{P-P} = 81$ Hz); $^{77}Se\{^1H\}$, −97.4 ppm ($\Delta_{1/2} = 40$ Hz; $^1J_{Se-P} = 610$ Hz); $^{139}La\{^1H\}$, 453 ppm ($\Delta_{1/2} = 2370$ Hz). These assignments are made from samples that were obtained from the controlled synthesis of what we believe is predominately compound **1** (see below). No absorption is present in the UV−vis spectrum between 230 and 800 nm.

$(C_5H_5)_2Gd[\eta^3\text{-}N(SePPh_2)_2]$, 2. A procedure similar to that used for **1** was employed to produce clear colorless crystals of **2**. Mp: 274 °C. Yield: 30%. Anal. Calcd for $C_{34}H_{30}GdNP_2Se_2$: C, 49.22; H, 3.64; N, 1.69. Found: C, 48.85; H, 3.67; N, 1.40. No resonance was found in the $^{31}P\{^1H\}$ NMR spectrum between −150 and 450 ppm. No absorption is present in the UV−vis spectrum between 230 and 800 nm.

$(C_5H_5)_2Er[\eta^3\text{-}N(SePPh_2)_2]$, 3. A procedure similar to that used for **1** was employed to produce pink crystals of **3**. Mp: 224 °C. Yield: 77%. Anal. Calcd for $C_{34}H_{30}ErNP_2Se_2$: C, 48.63; H, 3.60; N, 1.67. Found: C, 48.58; H, 3.41; N, 1.37. $^{31}P\{^1H\}$ NMR: 62.16 ppm (($\Delta_{1/2} = 25$ Hz; no satellites arising from the ^{77}Se atoms are visible). UV−vis (CH_2Cl_2 solution) nm (ϵ (M^{-1} cm^{-1})): 342, (407); 383, (207); 527,(114).

$(C_5H_5)_2Yb[\eta^2\text{-}N(SePPh_2)_2]$, 4. A procedure similar to that used for **1** was employed to produce orange crystals of **4**. Mp: 198−200 °C, to a red liquid. Yield: 81%. Anal. Calcd for $C_{34}H_{30}NP_2Se_2Yb$: C, 48.30; H, 3.58; N, 1.66. Found: C, 48.31; H, 3.89; N, 1.06. $^{31}P\{^1H\}$ NMR: 82.94 ppm ($\Delta_{1/2} = 25$ Hz; $^1J_{P-Se} = 566$ Hz). UV−vis (CH_2Cl_2 solution): shoulder at 390 nm.

$(C_5H_5)_2Yb[\eta^3\text{-}N(SPPh_2)_2]$, 5. A procedure similar to that used for **1** was employed to produce orange crystals of **5**. Mp: 228 °C to a red liquid. Yield: 57%. Anal. Calcd for $C_{34}H_{30}NP_2S_2Yb$: C, 54.32; H, 4.02; N, 1.86. Found: C, 54.53; H, 3.59; N, 1.87. $^{31}P\{^1H\}$ NMR: 74.1 ppm ($\Delta_{1/2} = 33$ Hz). UV−vis (CH_2Cl_2 solution): shoulder at 380 nm.

X-ray Crystallography. Crystals of **1**, **2**, **3**, **4**, and **5** were isolated under immersion oil in an N_2-filled crystal mounting box and were suspended in a Nylon loop before being rapidly frozen in the dry N_2 stream of a diffractometer for data collection. The crystal of **4** retains a THF molecule of crystallization. Data for all compounds were collected at −120 °C with a Bruker Smart CCD diffractometer with the use of graphite-monochromatized Mo Kα radiation ($\lambda = 0.710\ 73$ Å). Final unit-cell dimensions were obtained from 8192 reflections tallied during data processing. Data collections in the ω scan mode were performed with the SMART program.[13] Cell refinement and data reduction were applied with the use of the SAINT program.[13] Face-indexed numerical absorption corrections were applied for compounds **1**, **2**, **3**, and **4**.[13] The crystal for compound **5** was too small (all of the dimensions were <0.15 mm) to enable accurate measurement of its faces while it was mounted in the Nylon loop under oil; thus, a semiempirical ellipsoidal absorption correction was applied with the program SADABS.[13] This method relies on the high redundancy of the data set. Also, SADABS was applied to all of the data sets to address possible incident-beam anomalies (crystal decay, incident-beam absorption, and different generator settings among frames) through the assignment and smoothing of individual scale factors for each frame.[13] All of the structures were solved by standard Patterson methods and refined by full-matrix least-squares methods.[14] Compounds **1**, **2**, and **3** solve in $P\bar{1}$ with one complete molecule in the asymmetric unit. Compound **4** also solves in $P\bar{1}$, though the cell has two unique metal complexes and two unique solvent molecules (THF) in the asymmetric unit. A pseudocenter of symmetry between the two metal complexes occurs at $x = 0.999(5)$, $y = 0.544(8)$, and $z = 0.748(4)$ in the cell. Similarly, the two solvent molecules have a center of symmetry at $x = 0.992(6)$, $y = 0.02(2)$, and $z = 0.754(3)$ in the cell. The given unit cell does not transform into a higher symmetry cell, and the program MISSYM,[15] in the PLATON[16] suite of programs, does not find any higher symmetry from the atomic coordinates; the bonding seems to be approximately the same in the two unique species. The final models were restricted to anisotropic displacement parameters for all non-hydrogen atoms. Some hydrogen atoms were found in difference electron

(12) Wilkinson, G.; Birmingham, J. M. *J. Am. Chem. Soc.* **1954**, *76*, 6210.

(13) SMART, Version 5.054; Data Collection and SAINT-Plus, Version 6.0; Data Processing Software for the SMART System; Bruker Analytical X-ray Instruments, Inc.: Madison, WI, 1999.

(14) Sheldrick, G. M. SHELXTL PC, Version 5.0; An Integrated System for Solving, Refining, and Displaying Crystal Structures from Diffraction Data; Siemens Analytical X-ray Instruments, Inc.: Madison, WI, 1994.

(15) Le Page, Y. *J. Appl. Crystallogr.* **1987**, *20*, 264−269.

(16) Spek, A. L. *Acta Crystallogr., Sect. A: Found. Crystallogr.* **1990**, *46*, C34.

Table 1. Crystallographic Details for $Cp_2La[N(SePPh_2)_2]$ (**1**), $Cp_2Gd[N(SePPh_2)_2]$ (**2**), $Cp_2Er[N(SePPh_2)_2]$ (**3**), $Cp_2Yb[N(SePPh_2)_2]$ (**4**), and $Cp_2Yb[N(SPPh_2)_2]$ (**5**)

	1	**2**	**3**	**4**	**5**
form	$C_{34}H_{30}LaNP_2Se_2$	$C_{34}H_{30}GdNP_2Se_2$	$C_{34}H_{30}ErNP_2Se_2$	$C_{34}H_{30}YbNP_2Se_2{\cdot}C_4H_8O$	$C_{34}H_{30}NP_2S_2Yb$
fw	811.36	829.70	839.71	917.60	751.69
a (Å)	9.7959(10)	9.7130(14)	9.704(2)	12.087(4)	13.8799(18)
b (Å)	12.4134(13)	12.2659(17)	12.222(3)	12.429(4)	12.6747(16)
c (Å)	13.9077(14)	13.953(2)	13.980(4)	23.990(7)	17.180(2)
α (deg)	88.106(2)	88.062(2)	88.230(4)	89.406(5)	90
β (deg)	88.327(2)	87.613(2)	87.487(4)	86.368(5)	91.102(3)
γ (deg)	68.481(2)	69.041(2)	69.107(4)	81.664(5)	90
T (°C)	−120	−120	−120	−120	−120
V (Å^3)	1572.2(3)	1550.7(4)	1547.4(7)	3558.8(18)	3021.8(7)
d_{calcd} (g/cm^3)	1.714	1.777	1.802	1.713	1.652
space grp	$P\bar{1}$	$P\bar{1}$	$P\bar{1}$	$P\bar{1}$	$P2_1/n$
Z	2	2	2	4	4
indep reflns	7152	7056	7242	15296	7286
R(int)	0.0190	0.0327	0.0317	0.0274	0.0226
λ (Å)	0.710 73	0.710 73	0.710 73	0.710 73	0.710 73
linear abs coeff (cm^{-1})	38	46	52	48	34
$R_1(F)^a(F_o^2 > 2\sigma(F_o^2))$	0.0257	0.0323	0.0278	0.0321	0.0218
$R_w(F_o^2)^b$ (all data)	0.0631	0.0698	0.0704	0.0810	0.0609

^{a} $R_1(F) = \Sigma||F_o| - |F_c||/\Sigma|F_o|$. ^{b} $R_w(F_o^2) = [\Sigma\, w(F_o^2 - F_c^2)^2/\Sigma\, wF_o^4]^{1/2}$; $w^{-1} = \sigma^2(F_o^2) + (0.04F_o^2)^2$ for $F_o^2 \geq 0$; $w^{-1} = \sigma^2(F_o^2)$ for $F_o^2 \leq 0$.

Table 2. Selected Distances (Å) and Angles (deg) in $Cp_2La[N(SePPh_2)_2]$ (**1**), $Cp_2Gd[N(SePPh_2)_2]$ (**2**), $Cp_2Y[N(SePPh_2)_2]$, $Cp_2Er[N(SePPh_2)_2]$ (**3**), $Cp_2Yb[N(SePPh_2)_2]$ (**4**)[a], and $Cp_2Yb[N(SPPh_2)_2]$ (**5**)[b,c]

	1	**2**	$Cp_2Y[\eta^3\text{-}N(SePPh_2)_2]$	**3**	**4a**	**4b**	**5**
Ln(1)−Q(1)	3.1234(4)	3.0589(5)	3.0524(18)	3.0374(6)	2.8340(7)	2.8320(8)	2.9400(6)
Ln(1)−Q(2)	3.1311(4)	3.0492(6)	3.0528(13)	3.0198(8)	2.8254(8)	2.8139(7)	2.8818(6)
Ln(1)−N(1)	2.615(2)	2.495(3)	2.449(5)	2.446(2)			2.3735(16)
Ln(1)−Cp(1)	2.563	2.434	2.392	2.378	2.288	2.313	2.344
Ln(1)−Cp(2)	2.543	2.412	2.379	2.362	2.296	2.293	2.337
Ln(1)−P(1)	3.5073(7)	3.4072(11)	3.397(2)	3.3763(10)	3.9124(12)	3.8867(12)	3.3152(6)
Ln(1)−P(2)	3.4978(7)	3.4138(11)	3.378(2)	3.3793(10)	3.8865(12)	3.8502(12)	3.2516(6)
P(1)−N(1)	1.620(2)	1.628(3)	1.632(5)	1.630(2)	1.594(3)	1.589(3)	1.6238(17)
P(2)−N(1)	1.626(2)	1.626(3)	1.633(5)	1.625(2)	1.595(3)	1.588(3)	1.6267(17)
P(1)−Q(1)	2.1462(8)	2.1375(11)	2.1432(18)	2.1348(9)	2.1709(11)	2.1700(11)	1.9846(7)
P(2)−Q(2)	2.1473(7)	2.1422(11)	2.1406(19)	2.1450(9)	2.1726(12)	2.1735(11)	1.9857(7)
Q(1)−Ln(1)−Q(2)	124.668(9)	128.57(1)	129.54(3)	129.94(1)	93.70(3)	93.02(3)	129.00(2)
Cp(1)−Ln(1)−Cp(2)	124.3	125.7	126.0	126.0	127.0	128.1	126.3
P(1)−N(1)−P(2)	141.08(14)	53.27(2)	138.6(3)	138.96(16)	135.0(2)	138.0(2)	141.87(11)
Q(1)−P(1)−N(1)	106.26(8)	105.17(11)	104.33(17)	104.58(9)	117.72(12)	117.27(12)	103.51(6)
Q(2)−P(2)−N(1)	106.44(8)	104.98(11)	104.90(18)	104.18(9)	117.45(12)	117.26(12)	105.43(6)
Q(1)−Ln(1)−N(1)	63.01(4)	64.62(7)	64.96(11)	65.16(6)			63.64(4)
Q(2)−Ln(1)−N(1)	63.09(4)	64.75(7)	65.20(11)	65.40(6)			65.70(4)
C(11)−P(1)−C(17)	107.82(13)	104.98(19)	107.0(3)	104.77(14)	104.04(17)	104.46(17)	104.91(9)
C(23)−P(2)−C(29)	105.03(12)	107.64(19)	105.6(3)	107.15(14)	106.35(18)	109.03(17)	107.00(9)
Cp(1)−Ln(1)−N(1)	129.5	125.3	124.0	124.3			120.3
Cp(2)−Ln(1)−N(1)	106.1	109.0	110.0	109.6			113.4
Cp(1)−Ln(1)−Q_{av}	117.0	115.6	115.3	115.6	124.1	124.9	113.9
Cp(2)−Ln(1)−Q_{av}	118.7	118.7	118.7	118.4	108.9	107.0	119.8
Ln(1)−P(1)−C(11)	125.70(8)	134.14(14)	124.0(2)	133.63(10)	120.07(12)	115.10(11)	128.70(7)
Ln(1)−P(1)−C(17)	125.41(10)	119.81(13)	127.6(2)	120.49(10)	133.59(13)	138.03(13)	124.89(7)
Ln(1)−P(2)−C(23)	135.30(9)	124.02(13)	133.3(2)	123.78(9)	111.82(12)	108.65(11)	126.53(7)
Ln(1)−P(2)−C(29)	118.87(8)	126.98(14)	119.86(19)	127.62(11)	138.67(14)	139.62(13)	125.27(7)

[a] Compound **4** crystallizes with two independent molecules in the asymmetric unit (**4**a and **4**b), and hence the distances and angles are presented for both molecules. [b] Cp(1) and Cp(2) are the centroids of atoms C(1)−C(5) and atoms C(6)−C(10), respectively. [c] Q_{av} is the midpoint of the line connecting Q(1) and Q(2). Q = Se in **1**, **2**, **3**, and **4**. Q = S in **5**. Ln = La (**1**), Gd (**2**), Er (**3**), Yb (**4**), or Yb (**5**).

density maps, but all were ultimately generated in calculated positions and constrained with the use of a riding model. The isotropic displacement parameter for a given hydrogen atom was set 20% larger than the atom to which it is attached. Crystallographic data are listed in Table 1; selected bond distances and angles are listed in Table 2. Figure 1 shows a connectivity plot representative of compounds **1**, **2**, **3**, and **5**. Figure 2 shows the displacement ellipsoid plots of compounds **4** and **5**. The numbering scheme of Figure 2 is typical for all of the compounds reported.

Crystals having morphologies different from those of the chosen crystals were present in some of the isolated materials. An orange plate, having approximately the unit cell of **1**, **2**, and **3**, was also isolated from the reaction that produced the reported crystals for compound **5**, though only a preliminary crystal structure was obtained, which turned out to be that of the same material without the solvent molecules. (Crystal data for the second form of $Cp_2Yb[\eta^3\text{-}N(SPPh_2)_2]$: $YbS_2P_2NC_{34}H_{30}$, triclinic, $P\bar{1}$, $a = 9.645(6)$ Å, $b = 12.105(8)$ Å, $c = 13.938(9)$ Å, $\alpha = 87.37(1)°$, $\beta = 86.99(1)°$, $\gamma = 68.83(1)°$, $T = 153$ K, $V = 1514.8(2)$ Å^3, $Z = 2$). Furthermore, a second crystal type of the Er compound (**3**) was also isolated; its structure was the same as that which is presented here. (Crystal data for the second crystal of $Cp_2Er[\eta^3\text{-}N(SePPh_2)_2]$: $ErSe_2P_2NC_{34}H_{30}$, triclinic, $P\bar{1}$,

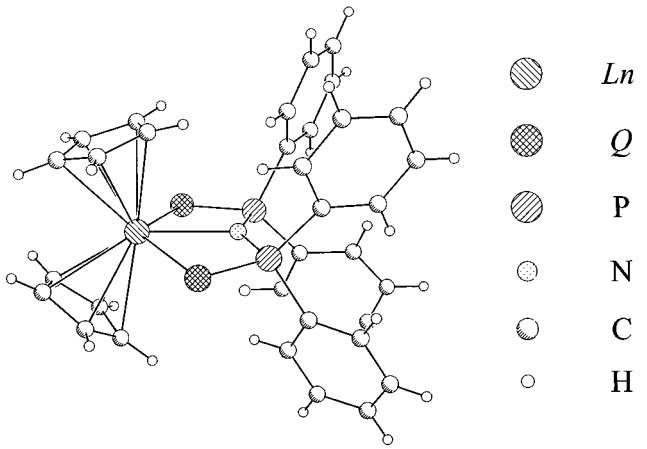

Figure 1. Connectivity plot of $Cp_2Ln[\eta^3\text{-}N(QPPh_2)_2]$ (Ln = La, Gd, or Er for Q = Se; Ln = Yb for Q = S). The H atoms shown are in idealized positions.

$a = 9.03(1)$ Å, $b = 10.34(2)$ Å, $c = 18.17(3)$ Å, $\alpha = 98.80(4)°$, $\beta = 96.54(3)°$, $\gamma = 110.53(3)°$, $T = 153$ K, $V = 1545.7(5)$ Å^3, $Z = 2$.) No effort was made to determine the factors controlling the various morphologies.

Results and Discussion

Syntheses. Reaction of 1:1 molar mixtures of Cp_3Ln and $HN(QPPh_2)_2$ in THF proceeds smoothly to produce $Cp_2Ln[N(QPPh_2)_2]$, as is outlined in reaction 1:

$$Cp_3Ln + HN(QPPh_2)_2 \rightarrow Cp_2Ln[N(QPPh_2)_2] + CpH \quad (1)$$

We recently described this reaction for Ln = Y.[1] For Ln = Y, La, and Gd, the reaction solutions remain colorless, whereas for Ln = Yb a dramatic color change from the dark green of Cp_3Yb to the bright orange of $Cp_2Yb[N(QPPh_2)_2]$ occurs as quickly as the compounds are added together. The pink color of Cp_3Er is similarly maintained by $Cp_2Er[N(SePPh_2)_2]$ (**3**). The UV−vis spectrum for **3** is shown in Figure 3. The ϵ values and shape of the absorptions are typical for fluorescent or $f-f$ transitions. All of the compounds are soluble in CH_2Cl_2 and THF and are stable for extended periods under inert conditions. Suitable crystals can be grown from THF solutions of compounds **1**, **2**, **3**, **4**, and **5** diluted with pentane or from cold concentrated CH_2Cl_2 solutions of the compounds. The melting points, though high for rare-earth chalcogenide compounds (range 198−274 °C), are not exceptional, given the known thermal stability of bis(cyclopentadienyl) rare-earth compounds.[17]

In the syntheses of compounds **2**, **3**, **4**, and **5**, the reactions proceed completely toward the monoligated species isolated, regardless of the amount of ligand added (see NMR Studies). If this reaction is governed by the relative acidities of the $HN(QPPh_2)_2$ and protonated Cp^-, then this observation implies that the $HN(QPPh_2)_2$ is not as acidic as the second protonated Cp ring on the Ln center. For **1**, however, the solution produced by adding 1 equiv of $HN(SePPh_2)_2$ to Cp_3La gave rise to multiple ^{77}Se and ^{31}P NMR resonances, and in addition to **1**, $Cp_3La(THF)$ crystallizes out, as confirmed by X-ray crystallography.[18] The elemental analysis does not coincide with $Cp_2La[N(SePPh_2)_2]$ (**1**) and is likely an average of a few products, including unreacted starting material. The high quality X-ray crystal structure of **1**, though, is presented in light of the other, more rational syntheses. A major peak in the ^{31}P NMR spectrum (37.1 ppm) is obtained when the reaction is carried out with slow addition (over 10 min) of $HN(SePPh_2)_2$ to the Cp_3La starting material. In the syntheses of the compounds **2**, **3**, **4**, and **5**, the rate of addition has no effect on the resultant NMR spectra.

Structures. The structures of compounds **1**, **2**, and **3** are very similar, with each comprising an $[N(QPPh_2)_2]^-$ ligand coordinated η^3 through two Q atoms and an N atom to a Cp_2Ln fragment. This same formally nine-coordinate geometry is seen with Ln = Y.[1] The structure of $Cp_2Ln[\eta^3\text{-}N(QPPh_2)_2]$ (Ln = La, Gd, Er for Q = Se; Ln = Yb for Q = S) is shown in Figure 1.

The structure of $Cp_2Yb[N(SePPh_2)_2]$, **4**, is different (Figure 2). Here, the ligand is connected η^2 through the two Se atoms; the Yb center is formally eight-coordinate. Apparently, the small radius of the Yb atom (1.04 Å versus 1.22 Å for La[19]) does not allow η^3-bonding from the ligand.

A similar steric argument could be made that the size of the chalcogen atom in the imidodiphosphinochalcogenido ligand controls whether the ligand coordinates η^2 or η^3 to the metal center. To address this point, we synthesized $Cp_2Yb[N(SPPh_2)_2]$ (**5**) and determined its structure (Figure 2). It turns out that **5** is isostructural with **1**, **2**, and **3** with η^3-coordination of the ligand to the metal center. Therefore, it seems as if an even smaller metal center may be necessary to force η^2-coordination from the imidodiphosphinosulfido ligand, at least in Cp_2Ln systems.

Important bond distances and angles for compounds **1**−**5** and $Cp_2Y[N(SePPh_2)_2]$[1] are summarized in Table 2. The Ln−Q distances range from 2.8320(8) Å in $Cp_2Yb[N(SePPh_2)_2]$ to 3.1311(4) Å in $Cp_2La[N(SePPh_2)_2]$. This difference of 0.2991(9) Å is much greater than the difference in the ionic radii of Yb (1.04 Å) and La (1.22 Å), although this is not surprising given the two distinct coordination modes of the ligand in these two species. The Yb−S distances in **5** (2.9400(6) Å and 2.8818(6) Å) are longer than that of 2.8263(8) Å in **4**, but again, this is the effect of a different coordination geometry. With the four selenide species and the Y compound recently synthesized,[1] it is possible to examine the relationship of the Ln−Se and Ln−N distances to the radius of the Ln atom. The line generated from the Ln−Se distances from the η^3-bound ligands in **1**, **2**, **3**, and $Cp_2Y[N(SePPh_2)_2]$ (top line in Figure 4) is

$$[\text{Ln−Se distance (Å)}] = 2.4(1) + 0.61(9)[\text{Ln radius (Å)}]$$

The Yb−Se distance in **4** is shown in the plot but was not used to generate the line, as the ligand is bound η^2 as opposed to η^3, as in the other compounds. A slope of 0.61(9) is less than that of 1.0, the value expected if the Ln−Se distances track directly with the radius of the Ln atom.

The Ln−N distances in the four η^3-bound ligands (2.615(2) Å, **1**; 2.495(3) Å, **2**; 2.446(2) Å, **3**; 2.3735(16) Å, **5**) are longer than would be expected for a nominal Ln−N single-bond distance in negatively charged N-containing species, such as $Y[N(SiMe_3)_2]_3$ (2.224(6) Å)[20] and $(C_6H_5CN)Y[N(SiMe_3)_2]_3$ (range 2.248(4) to 2.265(4) Å).[20] The Yb−N distance in the η^2-bound ligand in compound **4** is well out of the range of a bonding interaction. The Ln−N distances versus the radius of

(17) Bombieri, G.; Paolucci, G. In *Handbook on the Physics and Chemistry of Rare Earths*; Gschneidner, K. A., Jr., Eyring, L., Eds.; Elsevier Science B: 1988; Vol. 25, p 265.
(18) Rogers, R. D.; Atwood, J. L.; Emad, A.; Sikora, D. J.; Rausch, M. D. *J. Organomet. Chem.* **1981**, *216*, 383−392.
(19) Shannon, R. D. *Acta Crystallogr., Sect. A: Cryst. Phys., Diffr., Theor. Gen. Crystallogr.* **1976**, *32*, 751−767.
(20) Westerhausen, M.; Hartmann, M.; Pfitzner, A.; Schwarz, W. *Z. Anorg. Allg. Chem.* **1995**, *621*, 837−850.

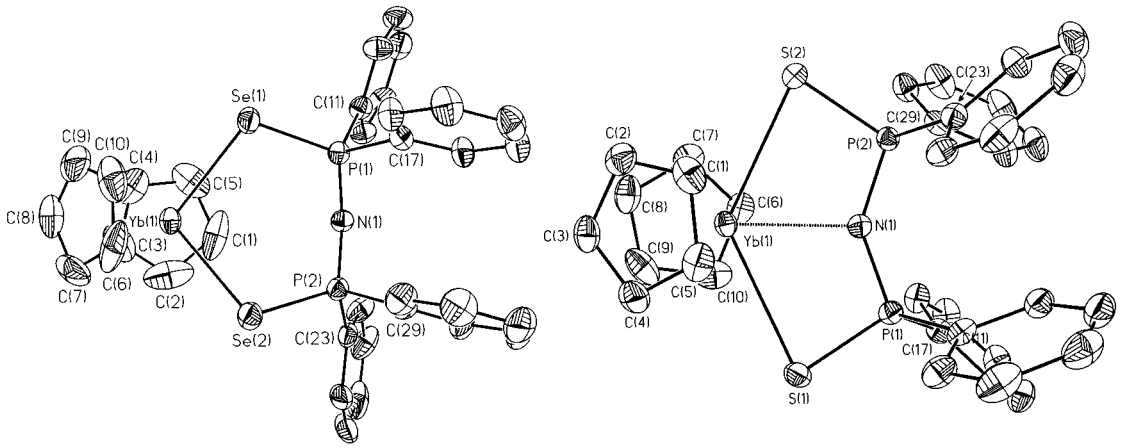

Figure 2. Displacement ellipsoid plots (50%) of $Cp_2Yb[\eta^2\text{-}N(SePPh_2)_2]$ (**4**) and $Cp_2Yb[\eta^3\text{-}N(SPPh_2)_2]$ (**5**) showing the atom numbering scheme. Similar structures and numbering exist in compounds **1**, **2**, **3**, and **5**. H atoms have been omitted for the sake of clarity.

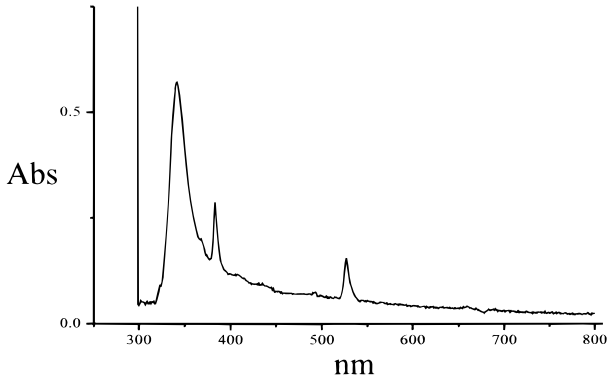

Figure 3. UV−vis spectrum of a sample of $Cp_2Er[N(SePPh_2)_2]$ (**3**) dissolved in CH_2Cl_2.

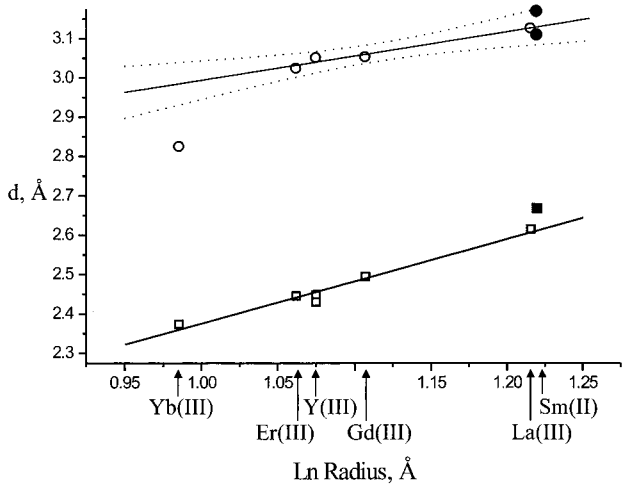

Figure 4. Plots of Ln radius vs Ln−Se (○) bond distances in **1**, **2**, **3**, **4**, and $Cp_2Y[N(SePPh_2)_2]$ and vs Ln−N (□) bond distances in **1**, **2**, **3**, **5**, $Cp_2Y[N(SPPh_2)_2]$, and $Cp_2Y[N(SePPh_2)_2]$. Sm−Se (●) and Sm−N (■) distances from $Sm[\eta^2\text{-}N(SePPh_2)_2][\eta^3\text{-}N(SePPh_2)_2](THF)_2$[23] are also shown, though not included in the calculations of the lines. The 95% confidence level in the top line is shown as two dotted lines. The errors on the bond distances fall within the width of the markers.

the Ln atom are plotted in Figure 4 for compounds **1**, **2**, **3**, **5**, $Cp_2Y[N(SPPh_2)_2]$, and $Cp_2Y[N(SePPh_2)_2]$.[1,19] The line generated from those points (bottom line in Figure 4) is

$$[\text{Ln}-\text{N distance (Å)}] = 1.3(1) + 1.07(9)[\text{Ln radius (Å)}]$$

Here, the slope is that expected for Ln−N distances tracking directly with Ln radius.

Scheme 2

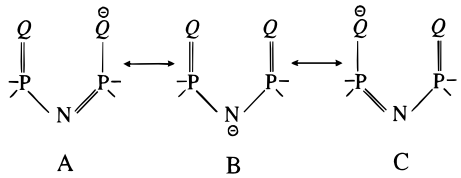

Whether or not the N atom is attached to the metal center creates markedly different bite angles (Q−Ln−Q) between the η^2- and η^3-bonding modes of the imidodiphosphinoselenido ligand. The Q−Ln−Q angle for the η^3-bound ligands of $Cp_2Y[N(SePPh_2)_2]$, **1**, **2**, **3**, and **5** averages 128(2)°, whereas this angle averages 93.36(3)° for the η^2-bound ligand in **4**.

In considering possible reasons for the difference in the structures of $Cp_2Yb[\eta^3\text{-}N(SPPh_2)_2]$ and $Cp_2Yb[\eta^2\text{-}N(SePPh_2)_2]$, let us first consider rare-earth complexes of the related imidodiphosphinooxido ligand, $[N(OPPh_2)_2]^-$. Known examples contain η^2-coordinated $[N(OPPh_2)_2]^-$, as in the structure of $Pr[N(OPPh_2)_2]_3$.[21] Here, the Pr center is not sterically saturated, as the acetone adduct $[Pr[N(OPPh_2)_2]_3(H_3COCH_3)]$ is easily synthesized from acetone solutions of the complex.[21] We believe that η^2-coordination of the oxido ligand arises from the increased electronegativity of the O atom (3.44) versus those of S (2.58) and Se (2.55).[22] Thus, in Scheme 2, the resonance structures A and C are more important for the oxido ligand. Localization of the electrons on the O atoms prevents the N atom from participating in the bonding. Resonance form B becomes more important as the electronegativity of the chalcogen atom is lowered, as for S and Se, and here the N atom, with a larger net negative charge, will bond to the metal center. Given the similar electronegativities of the S and Se atoms, it is tempting to argue that the difference in the structures of $Cp_2Yb[\eta^3\text{-}N(SPPh_2)_2]$ and $Cp_2Yb[\eta^2\text{-}N(SePPh_2)_2]$ arises from steric, rather than electronic, effects. S has a smaller radius than Se (1.84 Å vs 1.98 Å).[19] The late rare-earth element Yb may be too small to accommodate two Cp^- ligands, two Se atoms, and an N atom, but it may be able to accommodate the N atom if the smaller S atoms replace the Se atoms.

Although this argument in favor of steric effects might hold for Cp_2Ln complexes, it is certainly not general. Thus, the

(21) Platzer, N.; Rudler, H.; Alvarez, C.; Barkaoui, L.; Denise, B.; Goasdoué, N.; Rager, M.-N.; Vaissermann, J.; Daran, J.-C. *Bull. Soc. Chim. Fr.* **1995**, *132*, 95−113.

(22) Pauling, L. *The Nature of the Chemical Bond*, 3rd ed.; Cornell University Press: Ithaca, NY, 1960.

Table 3. Summary of Selected NMR Spectroscopic Data[a]

	no.	^{31}P	^{77}Se	$^{1}J_{P-Se}$	$^{2}J_{P-P}$	$\Delta_{1/2}$ in ^{31}P shift
$HN(SPPh_2)_2$		56.87				
$HN(SePPh_2)_2$		52.26	−163	790	25	
$Cp_2Y[N(SPPh_2)_2]$[1]		47.8				
$Cp_2Y[N(SePPh_2)_2]$[1]		41.03	−127	604	66	
$Cp_2La[N(SePPh_2)_2]$	**1**	37.1	−97	610, 613	81	25
$Cp_2Er[N(SePPh_2)_2]$	**3**	62.2				25
$Cp_2Yb[N(SePPh_2)_2]$	**4**	82.9		566		25
$Cp_2Yb[N(SPPh_2)_2]$	**5**	74.1				33

[a] NMR shifts are in ppm, coupling constants and the fwhm values ($\Delta_{1/2}$) are in Hz. All NMR spectra were collected on compounds dissolved in CD_2Cl_2. See Experimental Section for further details.

compound $Sm[\eta^2\text{-}N(SePPh_2)_2][\eta^3\text{-}N(SePPh_2)_2](THF)_2$ contains an η^2- and an η^3-$[N(SePPh_2)_2]^-$ ligand, but $Sm[\eta^2\text{-}N(SPPh_2)_2]_2(THF)_2$ contains only the η^2-$[N(SPPh_2)_2]^-$ ligand.[23] The Sm−Se and the Sm−N bond distances in the compound $Sm[\eta^2\text{-}N(SePPh_2)_2][\eta^3\text{-}N(SePPh_2)_2](THF)_2$ are plotted in Figure 4 as the filled spheres and the box, respectively. They fall within the 95% confidence limits of the line derived from the Cp_2Ln data and thus are not unusual. Therefore, on steric grounds, because the $N(SPPh_2)_2]_2^-$ ligand is η^2 in this system, one would certainly expect the $N(SePPh_2)_2]_2^-$ ligand also to be η^2. This Sm example is thus in striking contrast to the Cp_2Yb example above, if we assume that the solid-state structures are representative of the molecular structures in solution. We know this to be the case for the present structures (see below), but spectroscopic data bearing on this point are lacking (and are presumably impossible to obtain) for the Sm compounds.

NMR Studies. The ^{31}P NMR studies on compounds **1**−**5**, the starting materials $HN(SePPh_2)_2$ and $HN(SPPh_2)_2$, and $Cp_2Y[N(QPPh_2)_2]$ (Q = S, Se)[1] are summarized in Table 3. The ^{31}P NMR resonance of 52.3 ppm in $H[N(QPPh_2)_2]$ shows a diagnostic shift to a lower frequency of 37.1 ppm upon coordination of the ligand to the diamagnetic La center in $Cp_2La[N(SePPh_2)_2]$, **1**. This shift is similar to that in other compounds, such as $Cp_2Y[N(SPPh_2)_2]$ (47.8 ppm) and $Cp_2Y[N(SePPh_2)_2]$ (41.0 ppm).[1] The ^{31}P NMR resonance shifts in the paramagnetic compounds **3**, **4**, and **5**, however, are more difficult to interpret. In each, the resonance is shifted to a higher frequency, and additionally, it is broadened (see Table 3). The positions of the two Yb compounds **4** and **5** are also switched relative to the Y compounds. No resonance in the ^{31}P NMR spectrum of **2** was found. Only compounds **1** and **4** show P−Se coupling in the form of broadened satellites that surround the main peak. The $^{1}J_{P-Se}$ coupling values (613 Hz for **1**; 566 Hz for **4**) are less than that in the starting material (789 Hz) and imply a reduction in the P−Se bond order as the ligand is deprotonated. The two-bond P−P coupling, which is present during the time a single ^{77}Se atom makes the two ^{31}P atoms magnetically inequivalent (wherein one P atom is directly bonded to the ^{77}Se nucleus, and the other is three bonds away from it), is visible in the splitting of the satellites surrounding the main peak. The $^{2}J_{P-P}$ coupling of 81 Hz in **1** is similar to that in $Cp_2Y[N(SePPh_2)]$ ($^{2}J_{P-P}$ = 66 Hz). The dramatic increase in the $^{2}J_{P-P}$ coupling relative to the starting material ($^{2}J_{P-P}$ = 25 Hz for $HN(SePPh_2)_2$) arises from the near planarity of the ligand, which allows enhanced electron delocalization between the two P atoms. The values for the $^{2}J_{P-P}$ coupling imply that the η^3-coordination persists in solution in both the Y and the La selenide compounds. The $^{2}J_{P-La}$ coupling to the ^{139}La atom (^{139}La: spin = 7/2, 99.9% abundant) is not well resolved, but it does lead to broadening of all of the resonances.

The ^{77}Se NMR spectrum (^{77}Se: spin = 1/2, 7.8% abundant) of **1** was obtained. The spectrum shows a broadened doublet at −97.4 ppm, which is at a higher frequency than the resonance of the starting material ($HN(SePPh_2)_2$, δ = −163 ppm) and is nearer to that in $Cp_2Y[N(SePPh_2)_2]$ (δ = −127 ppm).[1] The large coupling arises from one-bond P−Se splitting ($^{1}J_{Se-P}$ = 610 Hz), which corresponds well to the coupling seen in the ^{31}P NMR spectrum. Once again, the peaks are further broadened by the one-bond coupling to the ^{139}La nucleus, although the expected octuplet is not resolved.

The addition of more than 1 equiv of $HN(SePPh_2)_2$ to Cp_3Ln (Ln = Yb, Gd, or Er) produces only the monosubstituted complexes $Cp_2Ln[N(SePPh_2)_2]$ and excess starting material. However, for compound Ln = La, **1**, this is not true. The addition of more than 1 equiv of $HN(SePPh_2)_2$ to Cp_3La produces multiple ^{31}P resonances at 33.1, 37.1, 41.2, and 48.9 ppm, in addition to resonances from the starting material (52.3 ppm). These are joined by three distinct ^{77}Se NMR resonances at −97.4 , −52.0 , and 24.2 ppm, in addition to the resonance from the starting material (−163 ppm). One ^{31}P resonance (37.1 ppm) and one ^{77}Se resonance (−97.4 ppm) can be ascribed to $Cp_2La[N(SePPh_2)_2]$, as deduced from spectra obtained from the controlled formation of predominantly compound **1** (see Syntheses section). Reaction conditions have not allowed the isolation of pure samples of the other compounds, but it is likely that the reaction proceeds further to give mixtures of $CpLa[N(SePPh_2)_2]_2$ and $La[N(SePPh_2)_2]_3$, in addition to leaving some unreacted starting material in the form of $Cp_3La(THF)$.[18] The ^{77}Se NMR resonance at 24.2 ppm is close to that for $Y[N(SePPh_2)_2]_3$ (34 ppm).[24]

Acknowledgment. This research was kindly supported by the National Science Foundation, Grant No. CHE-9819385.

Supporting Information Available: X-ray crystallographic files in CIF format for the structure determinations of the compounds $Cp_2Ln[N(QPPh_2)_2]$ (Ln = La (**1**), Gd (**2**), Er (**3**), or Yb (**4**) for Q = Se; Ln = Yb (**5**) for Q = S). This material is available free of charge via the Internet at http://pubs.acs.org.

IC990889O

(23) Geissinger, M.; Magull, J. *Z. Anorg. Allg. Chem.* **1997**, *623*, 755−761.

(24) Pernin, C. G.; Ibers, J. A. *Inorg. Chem.* **2000**, *39*, 1227−1237.